N89-20944

AERODYNAMIC ANALYSIS OF THREE ADVANCED CONFIGURATIONS USING THE TRANAIR FULL-POTENTIAL CODE

M. D. Madson, R. L. Carmichael, and J. P. Mendoza
NASA Ames Research Center, Moffett Field, California
Moffett Field, California

ABSTRACT

Computational results are presented for three advanced configurations: the F-16A with wing tip missiles and under-wing fuel tanks, the Oblique Wing Research Aircraft (OWRA), and an Advanced Turboprop research model. These results were generated by the latest version of the TranAir full-potential code, which solves for transonic flow over complex configurations. TranAir embeds a surface-paneled geometry definition in a uniform rectangular flow-field grid, thus avoiding the use of surface-conforming grids, and decoupling the grid generation process from the definition of the configuration. The new version of the code locally refines the uniform grid near the surface of the geometry, based on local panel size and/or user input. This method distributes the flow-field grid points much more efficiently than the previous version of the code, which solved for a grid that was uniform everywhere in the flow field. TranAir results are presented for the three configurations and are compared with wind tunnel data.

INTRODUCTION

The ability of linear potential panel method codes to compute flows about very general configurations has allowed them to be applied to a wide variety of configurations (Refs. 1-8). These codes give reliable results for configurations in which local flows do not deviate greatly from the freestream flow. For flows in the transonic regime, where both subsonic and supersonic flow exists, linear potential methods become inappropriate due to the violation of the small perturbation assumption. Nonlinear flow codes are required in order to predict transonic flows about aircraft, but are generally limited to relatively simple configurations due to "the difficulty in generating 'suitable grids' " (Ref. 9). Recent work (Refs. 10,11) has shown that improved grid generation techniques allow for increasingly complicated geometries to be analyzed. Unfortunately, simplifications to the actual geometry are generally required, as well as a good deal of time in generating the grid.

TranAir, a transonic full-potential code, utilizes the surface paneling technology of PANAIR (Refs. 12-15) in the definition of the computational model. The paneled definition of the configuration is then embedded in a relatively coarse rectangular array of flow-field grid points. The modeling generality afforded by the use of surface panels, and the decoupling of the flow-field grid definition from the definition of the geometry, allows TranAir to routinely solve transonic flow problems about very complex configurations.

The previous version of TranAir utilized a uniform grid which remained constant throughout the solution process. This uniform grid approach generally causes the grid to be much finer than necessary to predict the linear Prandtl-Glauert flow which prevails away from the geometry and not fine enough to adequately predict the rapidly changing flow properties near the surface of the geometry. The grid refinement capability allows the definition of a much coarser initial grid, so that the grid away from the boundary is not unnecessarily fine. The code then refines the initial uniform grid near the surface of the geometry where a finer grid is necessary in order to resolve the rapidly changing flow field. The refinements are based on local panel size and/or user input. The user may control the levels of refinement over regions of the geometry, thus controlling the distribution, and to some extent the number, of grid points generated for a given problem. The grid refinement capability generates a much more efficient grid upon which to obtain a solution. For

test cases analyzed by both the original uniform grid version and the new refined grid version of TranAir, the total number of grid points defined for the problem by the new version of the code was consistently 50% less than was defined by the previous version of TranAir, while at the same time yielding more accurate solutions.

DESCRIPTION OF THE METHOD

The TranAir program may be broken into three distinct sections: the input processor, the solver, and the output processor. A very brief description of each of these sections is presented here. A detailed description of the inner workings of the code, including the mathematics behind the solution process, is reserved for future publication.

Input Processor

The input processor reads the input file describing the configuration and flow conditions, checks the geometry for proper abutments and defines appropriate boundary unknowns and their locations. Most of the code for the input processor was taken directly from the pilotcode version of PANAIR. This helped in quickly producing reliable input processor code, as well as assuring compatability between PANAIR and TranAir input files.

Solver

The solver first defines an initial uniform grid about the input geometry based on values input by the user, who defines the minimum and maximum values of the grid in each direction, as well as the number of grid points in each direction. After setting up the initial grid, the solver successively refines the grid based on the size of the surface panels contained within each grid box. These refinements are limited to the neighborhood of the aircraft surface, and the user may control the minimum and maximum levels of the refinements. In addition, the user may specify a region (volume) of interest about portions of the geometry where additional control over the refinement is desired. Within this region, the user specifies minimum and maximum levels of refinement, which are independent of the refinements specified over the geometry outside of the region. In the near future, a solution–adaptive refinement capability will be introduced to allow grid refinement to be based on the current state of the solution to the system of equations.

Having produced a refined computational grid, the solver constructs finite element operators on that grid. A trilinear basis function for the potential is associated with each finite element. Discretized operators are obtained using the Bateman variational principle (Ref. 16) in a manner which is fully conservative and second–order accurate. This discretization yields a set of nonlinear algebraic equations which simulate the original full–potential partial differential equation. Operators in supersonic regions are altered using a first–order artificial dissipation for shock capturing.

The set of nonlinear algebraic equations is solved by an iterative process. An orthogonal direction algorithm called GMRES (Generalized Minimum RESidual) (Refs. 17,18) is used to drive the solution process in conjunction with multiple preconditioners. The preconditioners consist of a fast Poisson solver, which is particularly effective for regions where the flow remains subcritical, and an incomplete factorization of the sparse matrix produced by linearizing the set of nonlinear algebraic equations. The sparse matrix is defined by selecting a subset of the entire system of equations and by closing the set through the imposition of a Dirichlet boundary condition. This 'reduced set' of points consists of all finite element nodes which make up a refinement of a box on the global Cartesian grid plus all nodes which make up a finite element where the flow is supersonic. A nested dissection ordering based on the physical location of finite elements in the computational grid is used to order the sparse matrix system. The incompete factorization is performed by using a drop tolerance when factoring the sparse matrix. If any element is smaller than either of its diagonals by the value of the specified drop tolerance, it is set to zero. The preconditioners seem to work

more effectively in combination than would a single preconditioner by itself.

A significant advantage of the formulation is that the flow–field grid need only extend to a point where the flow is linear, rather than to a point where the flow is unperturbed. For cases in which there exist regions of supersonic flow, the flow–field grid must be large enough to include the supersonic regions. The equation solved about the perimeter of the grid changes from the nonlinear full–potential equation to the linear Prandtl–Glauert equation. The ends of the computational grid can be relatively close to the configuration because the unknowns defined on the global Cartesian grid consist of sources for the velocity potential. These sources exist on a grid which is theoretically infinite in extent, but the sources go to zero rapidly as a function of distance from boundary surfaces. In fact, the sources are generally weak in the entire computational domain except near shocks, surface boundaries and wakes. The potential induced by specified sources is computed efficiently by a convolution integral of the sources with a discrete exterior Green's function.

Output Processor

Once the solution process is completed, either by executing the maximum number of iterations specified by the user, or by reducing the value of the residual below a user specified minimum, the value of the potential at each grid point has been obtained. From these values, information about the flow both in the field and on the aircraft surface may be obtained. Velocities in the flow field and on the surface may be computed, from which the user may obtain forces and moments for the configuration, and pressure coefficients, streamlines, and Mach contours both in the field and on the surface of the geometry. One of the output options creates a file with all requested information about the flow at each point on the surface. A translator program may be written which loads the information in the output file into a database management system such as RIM (Relational Information Manager, Ref. 19), which in turn may be used to generate information for input to various 2–D and 3–D graphics programs and displays. Other files may be generated by TranAir, which can be read by PLOT3D (Ref. 20) a 3–D dynamic display graphics program which runs on a graphics workstation.

DESCRIPTIONS OF THE MODELS

Three configurations were modeled for which transonic results were desired. These models demonstrate the ability of TranAir to analyze complex geometries in the transonic flow regime. Descriptions of each of these configurations are presented below.

F–16A w/Wing Tip Missiles and Under–Wing Fuel Tanks

The TranAir model of the F-16A includes all the components of the actual geometry. The model also includes the geometry for an AIM-9 wing tip missile and launcher, and for a 370–gallon under–wing fuel tank and pylon. The complete F-16A definition is shown in Figure 1. Previous publications have presented TranAir results for the basic F-16A with no external stores (ref. 21), and with the addition of the 370–gallon underwing fuel tanks (ref. 22). The addition of the missile/launcher geometry to the definition of the F-16A shows the flexibility of TranAir in being able to quickly add complex pieces of geometry to an existing configuration and successfully analyze the new model.

The paneled definitions of the tip missile and launcher, and the fuel tank and pylon, were created on a Calma CAD/CAM machine based on blueprint drawings. The definition of the launcher and missile is true to the actual geometry with the exception of the small gap that exists between the missile and the launcher. For simplicity, this region was faired over. The fins on the missile were modeled as flat plates, which is very close to the shape of the actual fins. Wakes were defined from the trailing edge of the launcher, the base of the missile, and the trailing edges of all the fins. Wakes from the trailing edge of each of the forward fins were defined such that they ended at the leading edge of the corresponding aft fin. This was done to conserve the circulation generated by the forward set of fins. The launcher wake was connected to the outboard wing wake by a wake 'filler' network.

ORIGINAL PAGE IS
OF POOR QUALITY

The fuel tank and pylon were also modeled true to the actual geometry, with the exception of the fins on the aft portion of the fuel tank. The top fin was omitted in order to simplify the wake modeling process. Since there was no sideslip angle in the computations, this simplification was considered to be reasonable. The side fins were modeled as flat plates, which is very close in shape to the actual fins. The wake from the pylon passes through the horizontal tail, so the wake had to be broken into two wakes. One passes over the tail, and one passes under the tail. The paneling on the horizontal tail networks had to be modified slightly so that there were network abutments where the wakes intersect the upper and lower tail surfaces.

The wind tunnel model of the F-16A had a flowthrough nacelle. The TranAir model of the nacelle inlet is a network of porous panels, on which the boundary conditions are (1) the velocity on the upstream side of the panels is the normal component of the freestream velocity, and (2) the perturbation potential on the downstream side of the panels is zero. The nacelle exhaust is closed off by a network of panels in the same manner as the inlet. The boundary conditions used on this network are (1) the total potential is constant on the downstream side of the network, and (2) the perturbation potential is zero on the upstream side. The constant total potential on the downstream side combined with wake networks emanating from the afterbody perimeter cause the flow to separate smoothly from the afterbody, rather than turning through a right angle as would occur if the base panels were modeled with solid-surface boundary conditions (Fig. 18 from Ref. 12).

TranAir allows one-half of the geometry to be input for cases which have one plane of symmetry, such as the F-16A model. The right half of the F-16A definition is comprised of 6388 surface panels and 754 wake panels. The right half of the initial uniform grid for this case contained $33 \times 11 \times 17$ points in the x, y, and z directions, respectively. Regions (volumes) of interest were specified around the wing, the fuel tank, and the tip missile assembly. Within these three regions, a minimum of three levels of refinement were specified, with a maximum of four levels in the tank and missile regions, and five levels in the wing region. The final refined grid from which a solution was generated contained approximately 71,000 grid points, which is less than half of the total number of grid points used by the original version of TranAir to obtain previous F-16 results. A spanwise two-dimensional cut of the refined grid is shown in Figure 2. This figure shows the refinement of the grid around the wing, as well as the fuel tank and missile assemblies. The refinement around the leading edge of the wing was one to two levels finer than the station seen in Figure 2, which is nearer to the trailing edge.

Advanced Turboprop Research Aircraft

The Advanced Turboprop configuration is designed to cruise at $M_\infty = 0.8$ and $C_L = 0.5$. The wind tunnel model is a combination pressure and force model having an active propeller which is driven by a compressed air turbine housed in the nacelle. Since the propeller slipstream induces upwash on the wing inboard of the nacelle and downwash on the wing outboard of the nacelle, the wing definition included twist designed to compensate for these effects. As a result of the wing twist, the power-off (propeller removed) wing pressures outboard of the nacelle achieve a fairly high suction peak. Wind tunnel data was generated for both power-on and power-off cases in order to study the power effects for the model.

The TranAir model does not include the definition of the propeller, or any of the related slipstream effects. The paneled definition of the right hand side of the advanced turboprop model, as well as the symmetric left hand side, is shown in Figure 3. The paneling was created on a Calma CAD/CAM machine based on geometry information provided by McDonnell Douglas. The paneled definition of one-half of the symmetric configuration consists of 1019 surface panels and 96 wake panels.

The absence of any tail surfaces in the definition of the TranAir model is consistent with the design of the wind tunnel model. The TranAir model differs from the wind tunnel model in only one respect, at the nacelle exhaust nozzle. The vertical plane of the exhaust nozzle on the wind tunnel model faces slightly inboard. The TranAir model defined the exit plane to be parallel to the $y - z$ plane. The definition of wakes for this configuration was fairly standard, with wakes emanating from the wing trailing edge, and from the nacelle exhaust nozzle and the fuselage base.

The initial global grid box for this case, which was defined only for the right hand side of this symmetric configuration, contained 33 × 11 × 17 points in the x, y, and z directions, respectively. A region of interest was defined around the leading edge of the wing, and the rest of the wing. The leading edge region specified a minimum of four, and a maximum of five, levels of refinement. The aft region specified a minimum of three, and a maximum of five, levels of refinement. A region around the nacelle specified a mimimum of three, and a maximum of four, levels of refinement. A spanwise two-dimensional cut showing the refined grid across the fuselage, wing and nacelle is shown in Figure 4.

Oblique Wing Research Aircraft

NASA has studied the feasibility of using oblique wing airplanes for flight at transonic and low supersonic speeds for many years. Airplanes embodying this concept should prove useful for missions that require variable geometry configurations. In order to resolve some of the remaining uncertainties associated with the oblique wing concept, a proposal to convert the NASA Digital Fly-By-Wire Airplane to the Oblique Wing Research Aircraft was made. As part of the overall research program associated with this airplane, a detailed comparison of wind tunnel with theoretical results is being made. The original numerical calculations were generated by PANAIR, a linear potential flow code. The same paneled definition of the Oblique Wing configuration was analyzed by TranAir in an attempt to more accurately predict the characteristics of the oblique wing in transonic flow, particularly when the wing is swept.

The configuration studied here was tested in 1986 in the Ames 11- by 11-foot Transonic Wind Tunnel. The wing has subsequently undergone considerable redesign, particularly with respect to planform area. The wing was designed to have an area of 250 sq.ft. on the full scale airplane, with a span of 50 ft. The wind tunnel model is an 0.087 scale model of the wing attached to a model of the F-8 fuselage.

The paneled definition of the Oblique Wing model included the wing at a 30° sweep angle, the fuselage, empennage, and ventrals. The ventrals and the horizontal and vertical tails were modeled as thin (flat plate) surfaces. The wing definition was generated on a Calma CAD/CAM machine. The same numerical definition was used to generate both the TranAir model and wind tunnel model of the wing. The paneled configuration, shown in Figure 5, consists of 1134 surface panels and 175 wake panels. Most of the surface panels (750 out of 1134) are used in the definition of the wing, with the paneling on the fuselage and empennage being relatively coarse. Both sides of the configuration were defined due to the absence of a plane of symmetry for the configuration. Wake networks were attached to the trailing edges of all lifting surfaces, including the vertical tail. Since the configuration is asymmetric, the vertical tail may generate significant side force, even at zero sideslip, and thus the vertical tail wake could not be omitted from the definition. The wing wakes pass through the vertical tail, so the tail had to be defined by two networks which abut along the line defined by the wing wakes.

The initial global grid box for this case contained 33 × 17 × 11 points in the x, y, and z directions, respectively. This box enclosed both sides of the geometry, rather than just one-half of the geometry, due to the asymmetry of the configuration. A region of interest was defined around the wing, with a minimum of four, and a maximum six, levels of refinement. Regions were also defined at the wing tips, and at the horizontal and vertical tails. These regions specified lesser degrees of refinement than was specified for the wing. The final refined grid from which a solution was generated contained approximately 46,000 grid points. A streamwise two-dimensional cut showing the refined grid along the centerline of the geometry is shown in Figure 6. As can be seen, the grid is relatively coarse over most of the fuselage, and much finer in the vicinity of the wing.

RESULTS

Wind tunnel results were available for all three of the configurations presented. The F-16A and Advanced Turboprop wind tunnel models generated pressure data, as well as force and moment data. The Oblique

Wing wind tunnel model was a force model only. The TranAir results presented here were obtained on a Cray X-MP/48, using 32 million words of a 128 million word solid-state storage device (SSD). Comparisons of TranAir results with wind tunnel data are presented below.

F-16A w/Wing Tip Missiles and Under-Wing Fuel Tanks

As was mentioned previously, TranAir results for the F-16A using the original version of the code have been published (Refs. 21,22). The main conclusion from these results was that, due to machine memory limitations, the uniform grid scheme did not allow the grid to be fine enough to resolve the flow near leading edges and tips of lifting surfaces, even though as many as 200,000 grid points were used. For the F-16A configuration shown in Figure 1, the final refined grid generated by the new version of TranAir consisted of only 71,000 points. The TranAir predicted $C_p^{'s}$ for the F-16A with wing tip missiles and fuel tanks are shown in Figure 7 for $M_\infty = 0.6$ and $\alpha = 4°$.

The previously published wing pressure results showed reasonable agreement with wind tunnel data (Ref. 23) with two exceptions. Leading edge suction peaks were not captured because the grid was very coarse relative to the geometry. Also, pressures at the wing tip were in poor agreement with wind tunnel data. The poor agreement was due to both the relative coarseness of the grid at the tip, and the fact that no wind tunnel data existed for the F-16A without wing tip missiles and launchers.

The effect of adding the tip missile and launcher geometry to the definition of the F-16A, as well as the improved resolution of the flow due to the grid refinement capability, is evident in Figure 8. This figure shows wing tip C_p predictions from both versions of TranAir, as well as from wind tunnel data. The results from the original version of TranAir did not include the wing tip missiles and launchers in the definition of the geometry. The poor leading edge results, however, were caused by poor resolution of the grid in the region, rather than the absence of the missile geometry. Results from the new version of TranAir show much better agreement with wind tunnel data. This improvement in the predicted pressures can be attributed to both the addition of the missile/launcher geometry to the TranAir model and the grid refinement capability which more accurately resolves the flow in the region.

Advanced Turboprop Research Aircraft

Figure 9 shows the TranAir and wind tunnel C_p predictions for $M_\infty = 0.6$ and $\alpha = 2°$ at two wing stations. These results show TranAir predictions which are in reasonable agreement with wind tunnel data. The tap station shown in Figure 9a is inboard of the nacelle. The absence of a pressure peak near the leading edge reflects the negative twist inboard of the nacelle designed to offset the propeller upwash. Due to the spacing of the wing paneling on the computational model, TranAir results were not available at exactly the same tap station as the wind tunnel data. The closest available data on the TranAir model was 3% inboard from the wind tunnel station, which could explain the slight difference in C_p predictions between TranAir and wind tunnel data. The tap station in Figure 9b is outboard of the nacelle. The high suction peak reflected in the wind tunnel data is a result of the upward wing twist outboard of the nacelle designed to offset propeller downwash. TranAir results for the outboard tap station do not predict the magnitude of the suction peak. This is most likely due to the refined grid still being too coarse near the leading edge. Another possible explanation is the relative coarseness of the wing paneling. Both possibilities will be explored in future research. The TranAir C_p prediction over the entire configuration for $M_\infty = 0.6$ and $\alpha = 2°$ is shown in Figure 10.

Oblique Wing Research Aircraft

Results for the Oblique Wing geometry were obtained for $M_\infty = 0.8$ and $\alpha = 5°$, at a 30° wing sweep angle. Figure 11 shows the TranAir prediction of C_p for the entire configuration. Since no wind tunnel pressure data are available, this figure must be used to judge whether or not the predicted pressures seem reasonable.

Figure 12 shows plots of C_L and C_m vs. α, in which TranAir data are compared with wind tunnel data and PANAIR predictions. Although PANAIR results showed reasonable agreement with wind tunnel results, the effects of applying a linear potential code to a transonic flow problem are evident. These plots show that TranAir predictions compare much better with wind tunnel data than do the PANAIR predictions. The lift curve from the TranAir data is in good agreement with the wind tunnel curve, although the slopes differ slightly. The TranAir data was obtained with a relatively coarse flow–field grid (45,000 points), with the majority of points existing near the wing surface. By refining the grid more around the fuselage and the empennage, as well as the wing, a more accurate lift prediction should be possible.

The pitching moments predicted by TranAir were parallel to the wind tunnel data, and were closer to the wind tunnel data than the PANAIR prediction. The extrapolated value of the zero–lift pitching moment for TranAir differs by a significant amount. Several possible factors may contribute to this offset. The fuselage definition used for the PANAIR and TranAir models was not identical to the one used for the wind tunnel model. The nose region on the wind tunnel model of the F-8 fuselage has been modified several times over many years of testing, while the existing computational model retains the original definition of the nose. These modifications to the nose, besides affecting the aerodynamics of the fuselage, have made it difficult to maintain a reliable reference point on the fuselage. The location on the fuselage of the computational definition of the wing was approximated, and its distance from the horizontal tail could differ by a significant amount from that of the wind tunnel model. This possible discrepancy will be clarified and the proper adjustments to the computational model will be made. Another possible cause of pitching moment discrepancy is the modeling of the horizontal tail surfaces as flat plates. Future work will include the modeling of the tail surfaces with the same thickness as for the wind tunnel model.

It is encouraging that TranAir predictions for the transonic Mach no. are in better agreement with wind tunnel data than the linear potential predictions from the PANAIR code. Since, in the transonic flow regime, the flow violates the small perturbation assumption upon which linear potential flow is based, the PANAIR predictions should not be as accurate as those obtained by a nonlinear full–potential flow code such as TranAir.

FUTURE PLANS

Several enhancements are to be incorporated into the existing TranAir code. Some of these enhancements are in the implementation process, while others are scheduled to be completed by the end of the first quarter of 1989.

Most of the current effort is directed toward the implementation of a solution adaptive grid refinement capability. The current refinement method, which is based on local panel size and user input, requires a good deal of insight by the user as to where more grid points might be necessary in order to more accurately predict the flow in critical areas. Also, the refinement is limited to the neighborhood of the surface of the geometry. The solution adaptive refinement technique will evaluate the solution everywhere on the grid, and make further refinements in regions where the solution is less accurate. Refinements will also be allowed to extend into the flow field in order to accurately capture shocks.

The current code requires the freestream Mach no. to be less than 1.0. The flow field is allowed to have regions of supersonic flow, but the freestream value of the Mach no. must be subsonic. Near term effort will be directed toward implementing a supersonic freestream capability.

TranAir currently employs a trilinear basis function for the potential. This causes the velocity within a grid box to be approximately constant. Work is being done to implement a second–order basis function, which would then allow the velocity to vary across a grid box. This should combine with the grid refinement capability to improve the accuracy of the predictions.

Some effort will go into studying the feasibility of adding a 'viscous' term to the full–potential equation. This would enable the code to 'capture' wakes from sharp leading edges and trailing edges of lifting surfaces.

For the current version of TranAir, the user must define wakes in the same manner as required by linear potential flow codes. A wake-capturing capability would remove the burden of manual wake definition from the user, as well as more accurately defining the shape and location of the vortex sheets from the lifting surfaces.

SUMMARY

The TranAir full-potential code solves transonic flow problems about very general and complex configurations. A surface-paneled geometry definition is embedded in a uniform rectangular flow-field grid. This uniform grid is then refined in the neighborhood of the geometry based on the local surface panel size and/or user input. Finite element operators are constructed on the refined grid. Discretized operators are obtained in a conservative, second-order accurate fashion. A set of nonlinear algebraic equations which simulate the full-potential partial differential equation are generated, and are solved by an iterative process. Operators in supersonic regions are altered using a first-order artificial dissipation for shock capturing. TranAir results are shown for three different configurations: the F-16A with wing tip missiles and under-wing fuel tanks, the Oblique Wing Research Aircraft, and the Advanced Turboprop research model. These results demonstrate the ability of the code to routinely analyze complex configurations in the transonic flow regime. Future work will include the addition of a solution adaptive grid refinement capability, a higher-order basis function for the potential, a supersonic freestream capability, and the addition of a viscous term to the full-potential equation in order to capture wakes from sharp leading edges and trailing edges of lifting surfaces.

ACKNOWLEDGEMENTS

The TranAir code is being developed under NASA contract NAS2-12513 by the Boeing Military Airplane Company. The authors wish to thank F. T. Johnson, J. E. Bussoletti, S. S. Samant, D. P. Young, and R. G. Melvin for their dedicated work in the development of the TranAir code.

REFERENCES

[1] Madson, M. D., and Erickson, L. L., "Application of PAN AIR to an Advanced Supersonic Fighter/Attack Aircraft", AIAA Paper 85-4093, 1985.

[2] Snyder, L. D., and Erickson, L. L.,"PAN AIR Prediction of NASA Ames 12-Foot Pressure Wind Tunnel Interference on a Fighter Configuration", AIAA Paper 84-0219, 1984.

[3] Ghaffari, F., "PAN AIR Application to the F-106B", NASA Contractor Report 178165, 1986.

[4] Miller, S. G., and Youngblood, D. B., "Applications of USSAERO-B and the PAN AIR Production Code to the CDAF Model: A Canard/Wing Configuration", AIAA Paper 83-1829, 1983.

[5] van den Broek, G. J., "The Use of a Panel Method in the Prediction of External Store Separation", AIAA Journal of Aircraft Vol. 21, No. 5, May, 1984.

[6] Smith, B. E., and Ross, J. C., "Application of a Panel Method to Wake Vortex/Wing Interaction and Comparison with Experiment", AIAA Paper 84-2182, 1984.

[7] Fornasier, L., and Heiss, S., "Application of HISSS Panel Code to a Fighter-Type Aircraft Configuration at Subsonic and Supersonic Speeds", AIAA Paper 87-2619, 1987.

[8] Ross, J. C., "Applicability of a Panel Method, Which Includes Non Linear Effects, to a Forward-Swept-Wing Aircraft", AIAA Paper 84-2402, 1984.

[9] Holst, T. L., Slooff, J. W.,Yoshihara, H., and Ballhaus, W. F., Jr., "Applied Computational Transonic Aerodynamics", AGARD AG-266, 1982.

[10] Karman, S. L., Steinbrenner, J. P., and Kisielewski, K. M., "Analysis of the F-16 Flow Field by a Block Grid Euler Approach", AGARD Paper 18, 58th Meeting of the Fluid Dynamics Panel Symposium on Applications of Computational Fluid Dynamics in Aeronautics, 1986.

[11] Flores, J., Reznick, S. G., Holst, T. L., and Gundy, K., "Transonic Navier-Stokes Solutions for a Fighter-Like Configuration", AIAA Paper 87-0032, 1987.

[12] Carmichael, R. L., and Erickson, L. L., "PAN AIR - A Higher Order Panel Method for Predicting Subsonic or Supersonic Linear Potential Flows About Arbitrary Configurations", AIAA Paper 81-1255, 1981.

[13] Derbyshire, T., and Sidwell, K. W., "PAN AIR Summary Document (Version 1.0)", NASA CR-3250, 1982.

[14] Magnus, A. E., and Epton, M. A., "PAN AIR - A Computer Program for Predicting Subsonic or Supersonic Linear Potential Flows about Arbitrary Configurations using a Higher Order Panel Method (Version 1.0), Vol. I, Theory Document", NASA CR-3251, 1981.

[15] Sidwell, K. W., Baruah, P. K., and Bussoletti, J. E., "PAN AIR - A Computer Program for Predicting Subsonic or Supersonic Linear Potential Flows about Arbitrary Configurations using a Higher Order Panel Method (Version 1.0), Vol. II, User's Manual", NASA CR-3252, 1981.

[16] Bateman, H., "Irrotational Motion of a Compressible Inviscid Fluid", Proceedings of the National Academy of Sciences, Vol. 16, 1930, pp. 816-825.

[17] Wigton, L. B., Yu, N. J., and Young, D. P., "GMRES Acceleration of Computational Fluid Dynamics Codes", AIAA Paper 85-1494, 1985.

[18] Saad, Y. and Schultz, M. H., "GMRES: A Generalized Minimal RESidual Algorithm for Solving Non-symmetric Linear Systems", Research Rep. YALEU/DCS/RR-254, Aug. 1983.

[19] Fishwick, P. A., and Blackburn, C. L., "Managing Engineering Data Bases: The Relational Approach", Computers in Mechanical Engineering (Underlined), Vol. 1, No. 3, Jan. 1983, pp. 8-16.

[20] Buning, P. G., and Steger, J. L., "Graphics and Flow Visualization in Computational Fluid Dynamics", AIAA Paper 85-1507. 1985.

[21] Erickson, L. L., Madson, M. D., and Woo, A. C., "Application of the TranAir Full-Potential Code to Complete Configurations", ICAS Paper ICAS-86-1.3.5, 1986.

[22] Madson, M. D., "Transonic Analysis of the F-16A with Under-Wing Fuel Tanks: An Application of the TranAir Full-Potential Code", AIAA Paper 87-1198, 1987.

[23] Hammond, D. G., "Wind Tunnel Data Report, 1/9-Scale F-16 Pressure Loads Test, AEDC 16'T Test TF-397 (Phase I and II), Vol. II of VI", General Dynamics Report No. 16PR135, 1976.

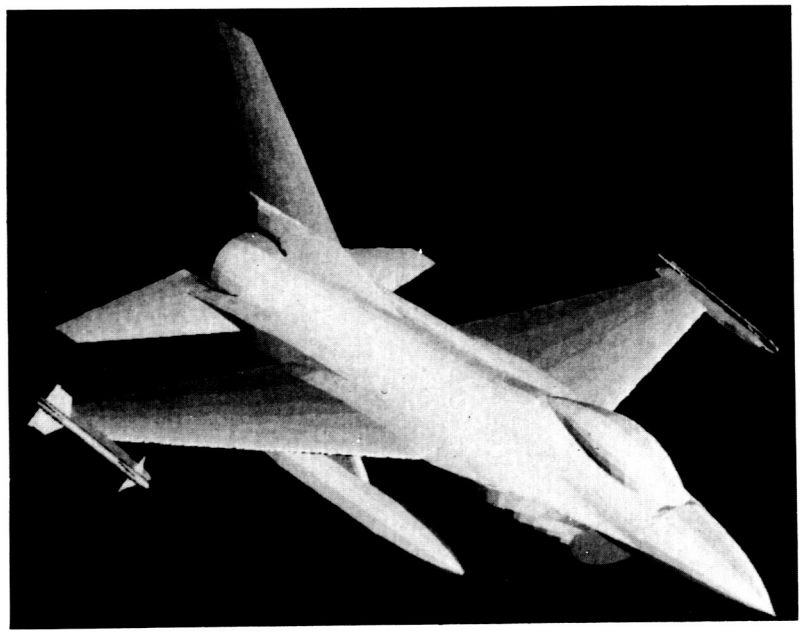

Figure 1. Surface panel definition of F-16A configured with wing tip missiles and under-wing fuel tanks.

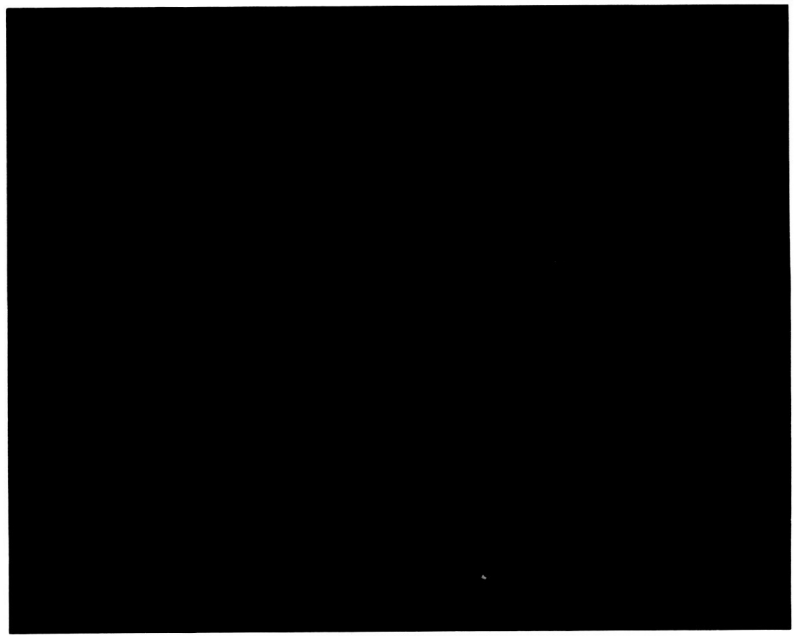

Figure 2. Spanwise two-dimensional cut of refined grid for F-16A configuration near wing trailing edge.

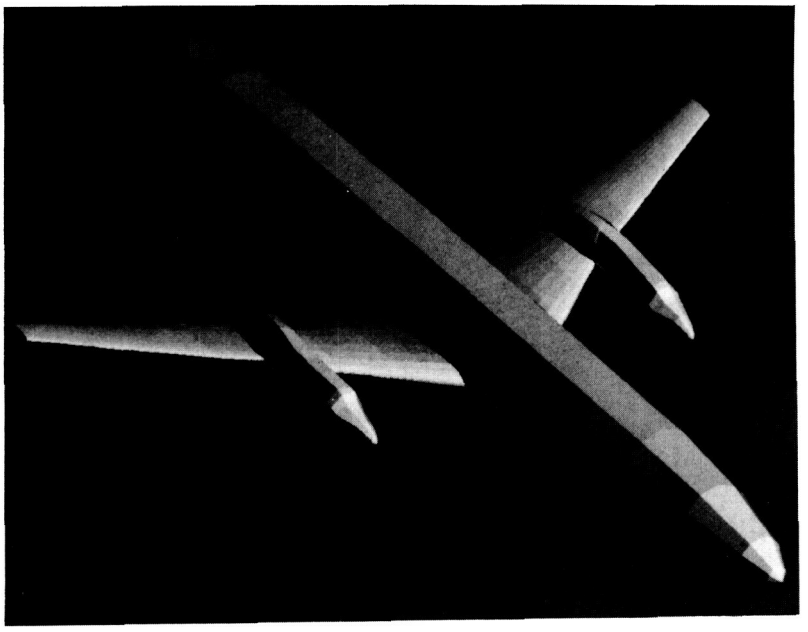

Figure 3. Surface panel definition of the Advanced Turboprop research model (ATP).

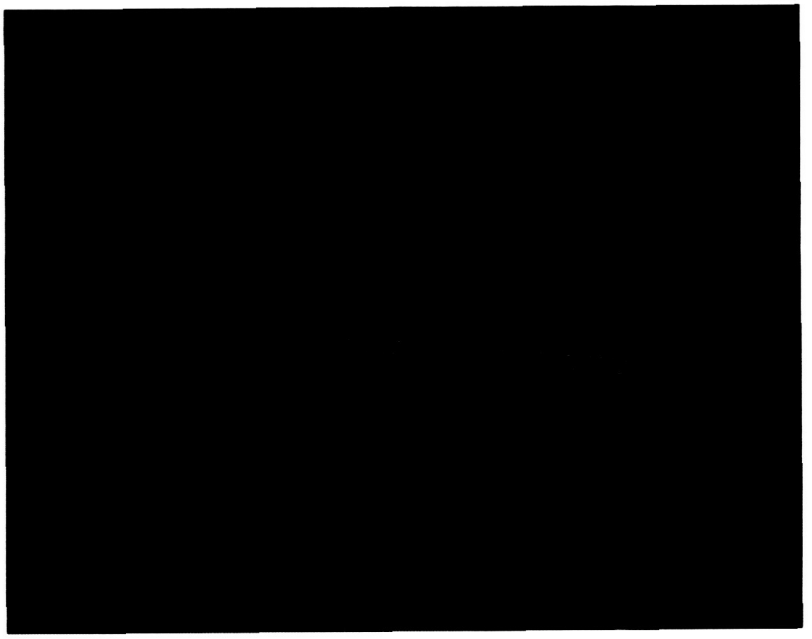

Figure 4. Spanwise two-dimensional cut of refined grid for the ATP through the wing/nacelle intersection.

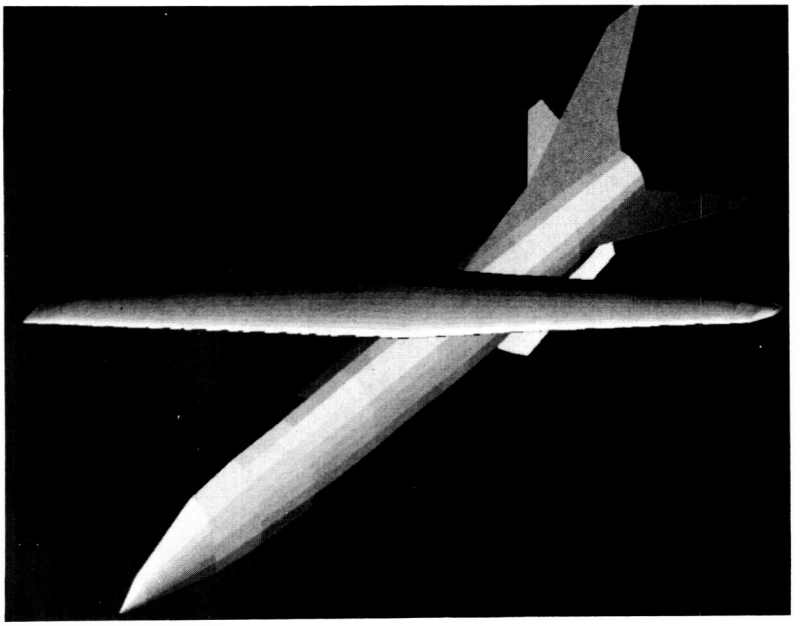

Figure 5. Surface panel definition of the Oblique Wing Research Aircraft (OWRA), wing sweep = 30°.

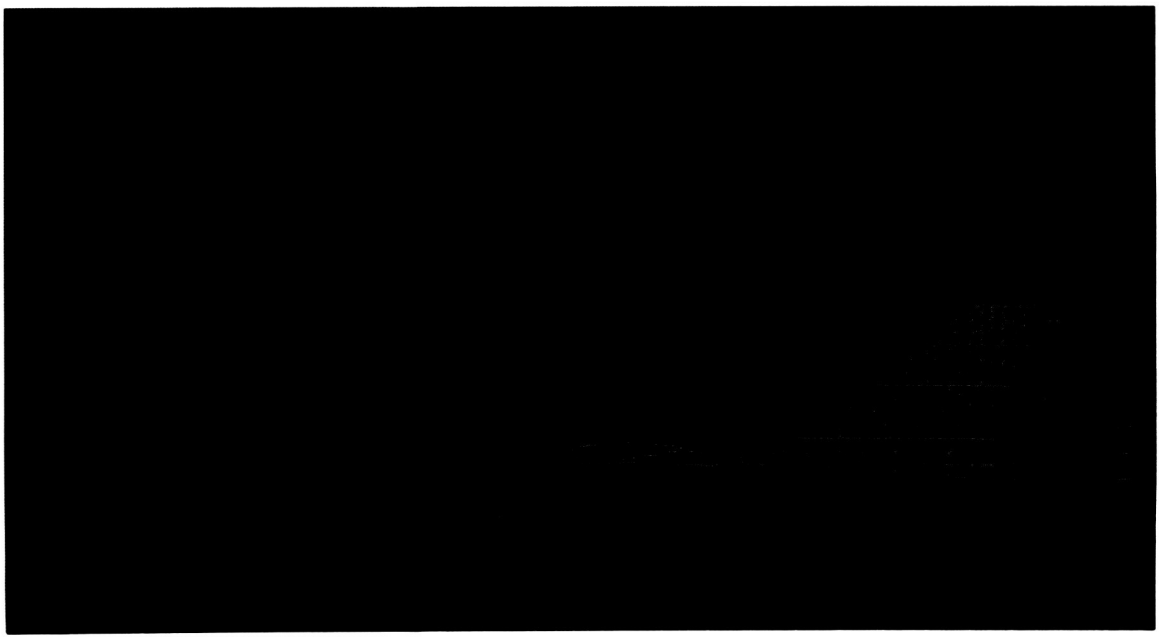

Figure 6. Streamwise two-dimensional cut of refined grid for the OWRA at the centerline of the configuration.

ORIGINAL PAGE
COLOR PHOTOGRAPH

Figure 7. TranAir C_p results for the F-16A, $M_\infty = 0.6$, $\alpha = 4°$.

F-16A w/Tip Missiles, Fuel Tanks
95% semi-span, $M_\infty = 0.6$, $\alpha = 4°$

SYMBOL
O Wind Tunnel Data
..... TranAir, Uniform Grid
——— TranAir, Refined Grid

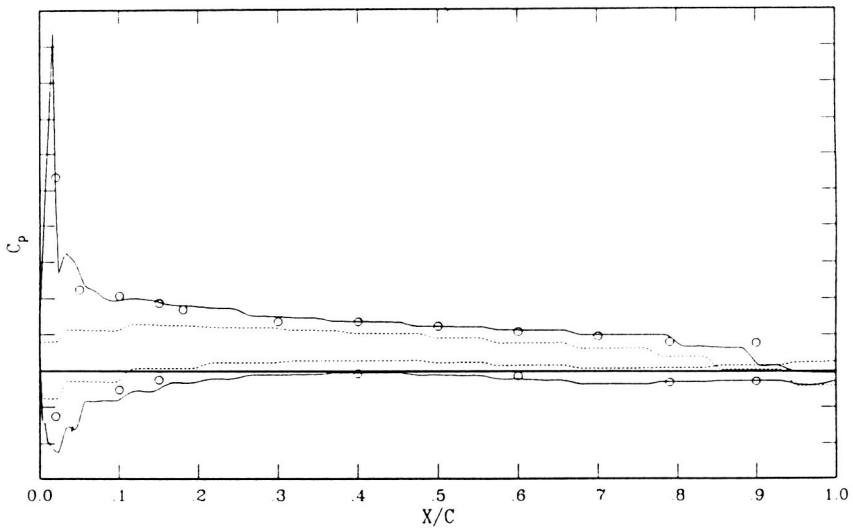

Figure 8. TranAir C_p results for the F-16A compared with wind tunnel data at 95% semi-span station, $M_\infty = 0.6$, $\alpha = 4°$.

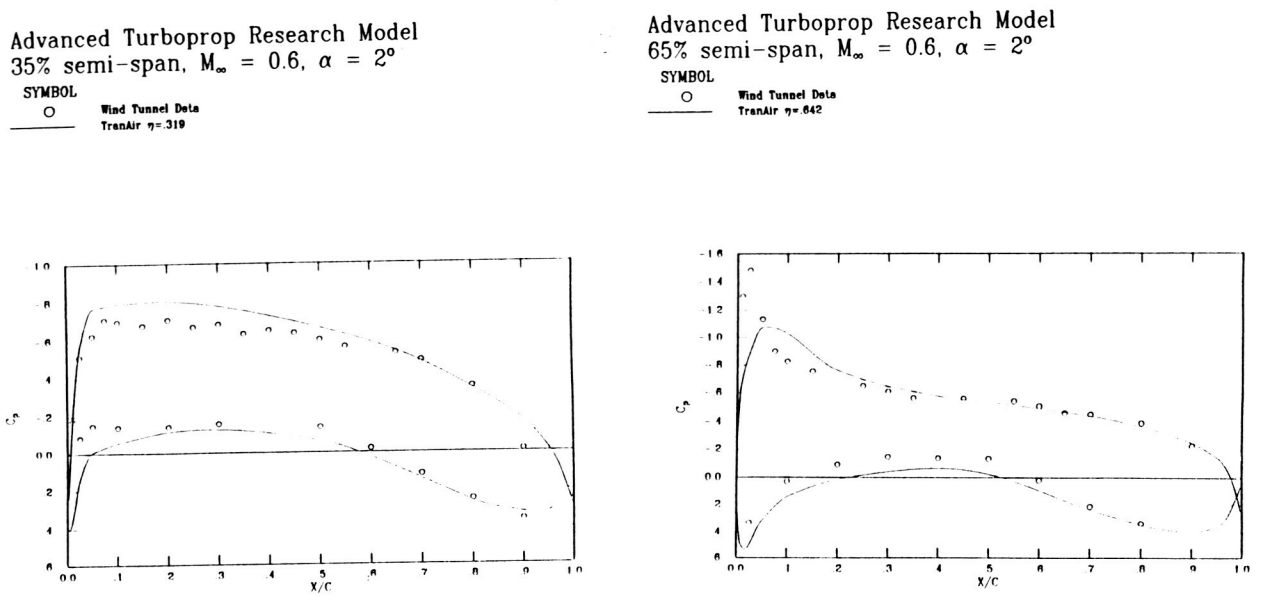

Figure 9. TranAir C_p results for the ATP compared with wind tunnel data, $M_\infty = 0.6$, $\alpha = 2°$.
a 35% semi-span station.
b. 65% semi-span station.

Figure 10. TranAir C_p results for the ATP, $M_\infty = 0.6$, $\alpha = 2°$.

ORIGINAL PAGE
COLOR PHOTOGRAPH

ORIGINAL PAGE
COLOR PHOTOGRAPH

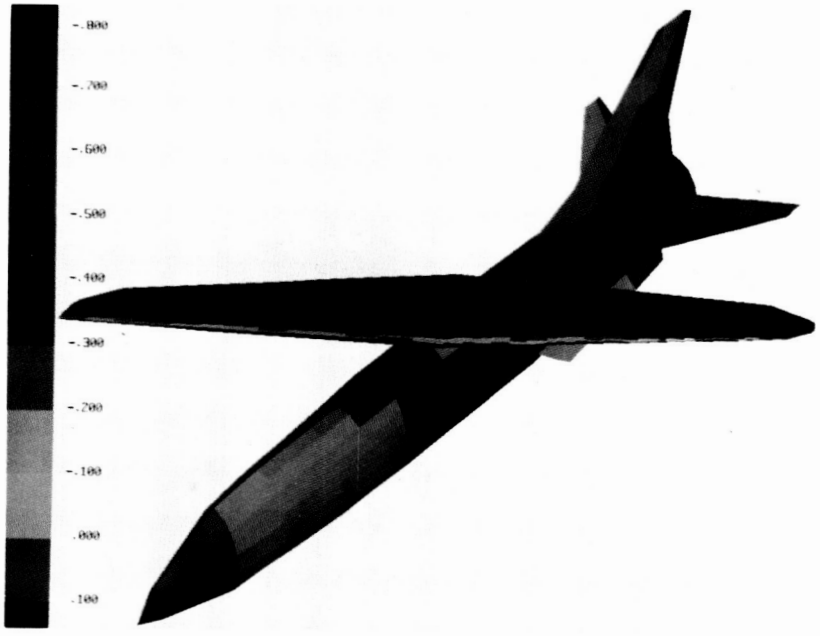

Figure 11. TranAir C_p results for the OWRA, $M_\infty = 0.8$, $\alpha = 5°$.

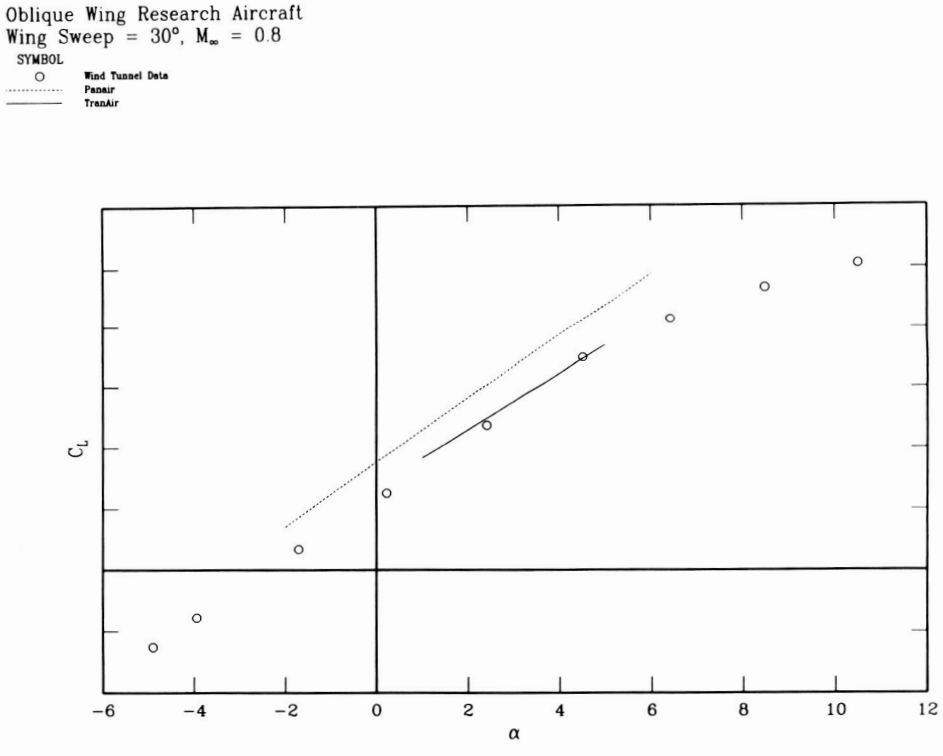

Figure 12. TranAir lift and pitching moment results for the OWRA compared with wind tunnel data, $M_\infty = 0.8$, $\alpha = 5°$.
a. Lift coefficient vs. angle-of-attack.

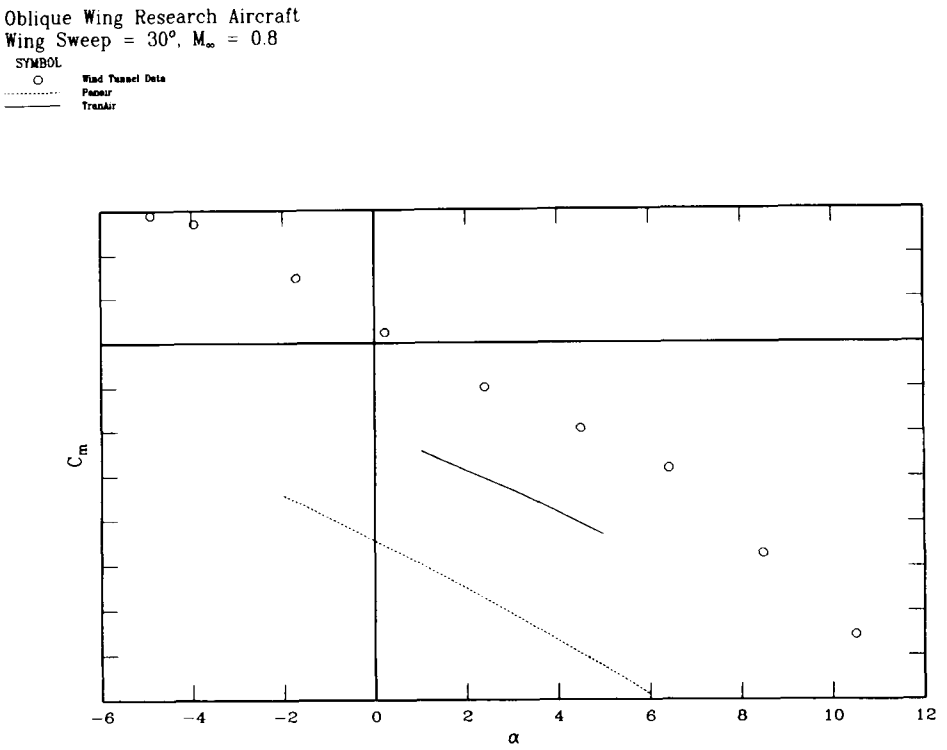

Figure 12. TranAir lift and pitching moment results for the OWRA compared with wind tunnel data, $M_\infty = 0.8$, $\alpha = 5°$.

b. Pitching moment vs. angle-of-attack.